

## Assessing the detail needed to capture rainfall-runoff dynamics with physics-based hydrologic response simulation

Benjamin B. Mirus,<sup>1,2</sup> Brian A. Ebel,<sup>1,3</sup> Christopher S. Heppner,<sup>1,4</sup> and Keith Loague<sup>1</sup>

Received 18 August 2010; revised 16 March 2011; accepted 5 April 2011; published 11 June 2011.

[1] Concept development simulation with distributed, physics-based models provides a quantitative approach for investigating runoff generation processes across environmental conditions. Disparities within data sets employed to design and parameterize boundary value problems used in heuristic simulation inevitably introduce various levels of bias. The objective was to evaluate the impact of boundary value problem complexity on process representation for different runoff generation mechanisms. The comprehensive physics-based hydrologic response model InHM has been employed to generate base case simulations for four well-characterized catchments. The C3 and CB catchments are located within steep, forested environments dominated by subsurface stormflow; the TW and R5 catchments are located in gently sloping rangeland environments dominated by Dunne and Horton overland flows. Observational details are well captured within all four of the base case simulations, but the characterization of soil depth, permeability, rainfall intensity, and evapotranspiration differs for each. These differences are investigated through the conversion of each base case into a reduced case scenario, all sharing the same level of complexity. Evaluation of how individual boundary value problem characteristics impact simulated runoff generation processes is facilitated by quantitative analysis of integrated and distributed responses at high spatial and temporal resolution. Generally, the base case reduction causes moderate changes in discharge and runoff patterns, with the dominant process remaining unchanged. Moderate differences between the base and reduced cases highlight the importance of detailed field observations for parameterizing and evaluating physics-based models. Overall, similarities between the base and reduced cases indicate that the simpler boundary value problems may be useful for concept development simulation to investigate fundamental controls on the spectrum of runoff generation mechanisms.

**Citation:** Mirus, B. B., B. A. Ebel, C. S. Heppner, and K. Loague (2011), Assessing the detail needed to capture rainfall-runoff dynamics with physics-based hydrologic response simulation, *Water Resour. Res.*, 47, W00H10, doi:10.1029/2010WR009906.

### 1. Introduction

[2] The ability to understand, quantify, and employ our knowledge of surface and near-surface hydrologic processes is critical for important environmental problems such as flooding, pollution, and ecosystem health. In small, headwater catchments it remains difficult to predict the flashy response to individual precipitation events. Rainfall-runoff dynamics may be dominated by subsurface stormflow [Hewlett and Hibbert, 1963] or by overland flow generated via the Horton mechanism of infiltration excess [Horton, 1945], the Dunne mechanism of saturation excess [Dunne and Black, 1970a, 1970b], or some combination thereof [Loague *et al.*, 2010]. The environmental controls on these different runoff generation processes are illustrated quali-

tatively in Figure 1. The original version of Figure 1 was assembled by Dunne [1978] on the basis of an extensive examination of data sets from a variety of catchments around the world. One problem with quantitatively comparing hydrologic response across different environmental conditions is that features such as climate, catchment size and geometry, geologic substrate, and vegetation cover are all interrelated and differ widely between sites. These differences are often compounded by significant heterogeneities within a given study area. Controls on the thresholds between the processes in Figure 1 remain difficult to define quantitatively because of the complexity of nonlinear dynamic interactions between climate, topography, soil hydraulic properties, vegetation, and land use. This study is motivated by the need for modeling tools that can be used to examine quantitative thresholds between different runoff generation mechanisms for a range of environmental conditions.

[3] Recent advances in computing power have facilitated the emergence of a new generation of physics-based hydrologic response models [e.g., VanderKwaak, 1999; Morita and Yen, 2002; Ivanov *et al.*, 2004; Panday and Huyakorn, 2004; Therrien *et al.*, 2004; Kollet and Maxwell, 2006; Qu and Duffy, 2007], developed in the spirit of the blueprint

<sup>1</sup>Department of Geological and Environmental Sciences, Stanford University, Stanford, California, USA.

<sup>2</sup>Now at U.S. Geological Survey, Menlo Park, California, USA.

<sup>3</sup>Now at U.S. Geological Survey, Boulder, Colorado, USA.

<sup>4</sup>Now at Eler and Kalinowski, Inc., Burlingame, California, USA.

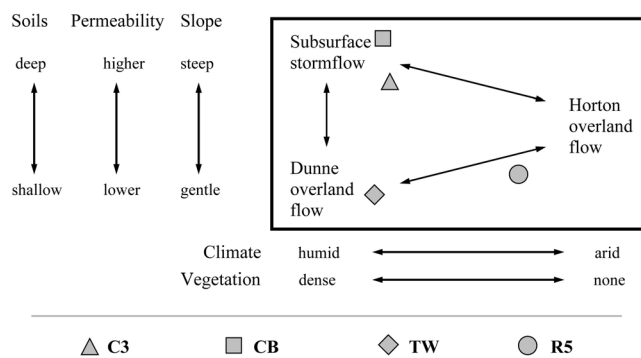


**Figure 1.** Environmental controls on the runoff generation mechanisms [after *Dunne*, 1978]. The C3, CB, TW, and R5 catchments are plotted schematically according to the dominant response mechanism(s).

outlined by *Freeze and Harlan* [1969]. These comprehensive models are all capable of simulating the range of runoff generation processes illustrated in Figure 1. Accompanying the increased complexity represented by this new generation of models are the correspondingly extensive data requirements for adequate parameterization of boundary value problems [see *Freeze and Cherry*, 1979] and evaluating model performance. Previous simulation-based efforts have highlighted the importance of considering observations of both integrated and distributed hydrologic response for achieving greater confidence in model results [*Refsgaard*, 2000] and limiting problems of equifinality [*Ebel and Loague*, 2006]. The scarcity of the distributed hydrologic response data sets appropriate for use with these sophisticated models remains the primary obstacle to their widespread application. Variability in the level of detail available to develop model boundary value problems for different study locations also presents an impediment to establishing acceptable metrics for performance of a given model and its intended application.

[4] *Kampf and Burges* [2007] provide a review of hydrologic response modeling and propose a framework for classifying and comparing distributed models. While many simpler rainfall-runoff models were designed primarily for operational applications, comprehensive physics-based models can also be employed to generate hypothetical realities for concept development and model testing [*Loague and VanderKwaak*, 2004; *Loague et al.*, 2006, 2010; *Ebel and Loague*, 2008; *Mirus et al.*, 2009a]. Such simulation-based approaches can be useful because they provide higher spatial and temporal resolutions than can be obtained with current field measurement capabilities.

[5] In the past decade, comprehensive physics-based hydrologic response models have been applied for a variety of quantitative studies investigating the surface and subsurface controls on runoff generation [*VanderKwaak and Loague*, 2001; *Morita and Yen*, 2002; *Loague et al.*, 2005; *Ebel et al.*, 2007b, 2008; *Heppner et al.*, 2007; *Qu and Duffy*, 2007; *Vivoni et al.*, 2007; *Jones et al.*, 2008; *Kollet and Maxwell*, 2008; *Li et al.*, 2008; *Mirus et al.*, 2007, 2009a]. In each of these studies, simulations were designed after a particular location or setting; each boundary value problem was parameterized and evaluated using data sets with disparate degrees of detail. Collectively, these efforts demonstrate how physics-based models can be employed for simulating runoff

generation processes across a range of environmental conditions over different spatial and temporal scales. However, the disparities between the data sets employed to establish the boundary value problems in these studies introduce various levels of bias that should be addressed.

[6] The difficulty in measuring small-scale heterogeneities of, for example, soil hydraulic properties and rainfall characteristics limits the utility of comprehensive distributed models [*McDonnell et al.*, 2007]. Improved understanding of how heterogeneity and disparities between different data sets impact simulated process representation is needed for designing networks of distributed measurements sufficient for adequately parameterizing and evaluating comprehensive physics-based models. Ultimately, better quantitative characterization of how surface-subsurface water interactions influence process thresholds may also promote more effective use of simpler rainfall-runoff models. Although important, the impacts of the topography or resolution of finite element meshes on simulated hydrologic response [e.g., *Vivoni et al.*, 2005] are not the focus of the effort presented herein.

[7] The objective of this work was to establish a common level of complexity for a distributed physics-based model, such that it can be employed without observational bias to quantitatively investigate the controls on runoff generation mechanisms across the range of environmental conditions illustrated in Figure 1. At the heart of this effort is the comprehensive, physics-based Integrated Hydrology Model (InHM), which has been used previously to generate base case boundary value problems for four well-characterized experimental catchments. In the context of the work presented here, the term boundary value problem [see *Freeze and Cherry*, 1979] refers to (1) the size and shape of the region of flow, (2) the boundary conditions around the boundaries of the region, (3) the initial conditions in the region, (4) the spatial distribution of the hydrogeologic parameters that control the flow, (5) the equations of flow within the region, and (6) a mathematical method of solution. Whereas characteristics 5 and 6 are incorporated within the framework of InHM, characteristics 1–4 were determined on the basis of available observations from the four base case catchments. The focus of this work is largely on characteristics 2 and 4 because the base case data sets for these four experimental catchments differ in terms of the characterization of spatial and/or temporal variability in rainfall intensity, permeability, and soil depth; there is also a first-cut consideration for evapotranspiration and hysteretic water retention curves in some of the comparisons. The four base case boundary value problems are each reduced to a common level of simplicity to remove the bias from differences between the four data sets. The simulated impact of the boundary value problem characteristics, associated with different degrees of observational detail, are evaluated in terms of both the integrated and distributed hydrologic response.

[8] The focus of this work differs somewhat from previous simulation-based efforts to investigate the hydrologic response impacts of observational detail [e.g., *Loague*, 1988] and model complexity [e.g., *Loague*, 1992]. Each of the base cases employed in this study used all the observational details available to successfully capture a realistic (albeit not perfect) representation of hydrologic response with InHM. Each reduced scenario developed herein is intended to represent a fundamental response type, corresponding to one possible set of processes that can occur in real systems. The hypothesis

**Table 1.** Characteristics of the Four Base Case Experimental Catchments

Catchment	Location	Climate, Land Use	Drainage Area (ha)	Average Slope (deg)	Dominant Runoff Generation Mechanism <sup>a</sup>	References
C3	Oregon Cascades	semihumid, timber	1.7	18	SSSF	<i>Wemple</i> [1998], <i>Dutton</i> [2000], <i>Dutton et al.</i> [2005], and <i>Mirus et al.</i> [2007]
CB	Oregon Coast Range	humid, timber	0.1	43	SSSF	<i>Anderson et al.</i> [1997a, 1997b], <i>Montgomery et al.</i> [1997], <i>Torres et al.</i> [1998], and <i>Ebel et al.</i> [2007a, 2007b]
TW	southeastern Australia	temperate, grazing	10.5	3	DOF	<i>Western and Grayson</i> [1998] and <i>Mirus et al.</i> [2009a]
R5	central Oklahoma	semiarid, grazing	9.6	2	HOF/DOF	<i>Loague</i> [1986], <i>VanderKwaak</i> and <i>Loague</i> [2001], <i>Loague et al.</i> [2005], <i>Heppner et al.</i> [2007], and <i>Heppner and Loague</i> [2008]

<sup>a</sup>SSSF, subsurface stormflow; HOF, Horton overland flow; DOF, Dunne overland flow.

tested is that a simplified boundary value problem, with the various degrees of observational detail removed, will still be useful for representing the different runoff generation mechanisms.

## 2. The Integrated Hydrology Model

[9] The Integrated Hydrology Model (InHM) was developed [*VanderKwaak*, 1999] to quantitatively simulate, in a fully coupled approach, 3-D variably saturated flow and solute transport in porous media and 2-D flow and solute transport over the surface and in open channels. The most important characteristic of InHM related to the objectives of this work is that it requires no a priori assumption of a specific runoff generation mechanism. Infiltration and exfiltration rates are determined by spatially variable subsurface properties, spatially and temporally variable subsurface pressure head gradients, and spatially and temporally variable surface water depths. The governing equations are discretized in space using the control volume finite element method, and each coupled system of nonlinear equations in an InHM simulation is solved implicitly using Newton iteration. The full set of equations and a complete description of the details regarding the nuances of InHM are given by *VanderKwaak* [1999].

## 3. Catchment-Scale Data Sets

[10] The foundations for the simulations in this study are the base case boundary value problems, which were developed previously for InHM using data from four field sites: (1) the C3 catchment, Oregon, (2) the Coos Bay catchment, Oregon, (3) the Tarrawarra catchment, Australia, and (4) the R5 catchment, Oklahoma. The general characteristics of the four base case catchments are summarized in Table 1; the four catchments are also placed on Figure 1 in terms of their dominant runoff generation mechanisms. Perusal of Table 1 and Figure 1 illustrates that the four catchments were selected to represent the range of known mechanisms. While the data sets for these four catchments contain different degrees of information on rainfall and evapotranspiration, geology, soils, runoff, and near-surface soil hydraulic properties, all were suitable for adequately parameterizing and

testing InHM. The data used to establish the four base case boundary value problems are summarized in Table 2. Perusal of Table 2 illustrates the discrepancies between the degrees to which spatial variability in hydrologic response was characterized at the four sites. Details of the rigorous model performance evaluation using the continuous observations of both integrated and distributed hydrologic response summarized in Table 2 are provided elsewhere [*VanderKwaak and Loague*, 2001; *Loague et al.*, 2005; *Ebel and Loague*, 2006; *Mirus et al.*, 2007; *Ebel et al.*, 2007a, 2007b, 2008; *Heppner et al.*, 2007; *Mirus et al.*, 2009a]. Together, these four base cases provide an opportunity for concept development simulations to examine different levels of boundary value problem complexity across a variety of environmental conditions.

### 3.1. The C3 Base Case Boundary Value Problem

[11] The catchment known as C3 is located in the H. J. Andrews Experimental Forest in the Oregon Cascades. The C3 catchment is 1.7 ha in area, is steep (18°), and is

**Table 2.** Summary of the Data Sets Used to Establish the C3, CB, TW, and R5 Base Case Boundary Value Problems

Data Set Characteristic	C3	CB	TW	R5
Discharge <sup>a</sup>	1	2 <sup>b</sup>	1	1
Rain gauges	1	148	1	1
Piezometers	5	223	74	0
Tensiometers	1	100	0	0
Soil water content				
Neutron probe <sup>c</sup>	0	0	20	32
TDR <sup>d</sup>	108	42	665 <sup>e</sup>	0
Infiltration experiments/slug tests	48	177	42	247
Soil texture	9	3	125	247
Soil depth	9	630	125	247
Characteristic curves <sup>f</sup>	1	6	0	0

<sup>a</sup>Number of weirs, flumes, or culverts monitored using calibrated stage-discharge relationships.

<sup>b</sup>Upper and lower weirs.

<sup>c</sup>Number of locations in (x, y) with multiple depth measurements.

<sup>d</sup>Number of waveguide pairs.

<sup>e</sup>Mean number of measurement locations, made with the same equipment for 13 surveys [see *Western and Grayson*, 1998].

<sup>f</sup>Water retention and unsaturated hydraulic conductivity relationships estimated using in situ methods [see *Torres et al.*, 1998].

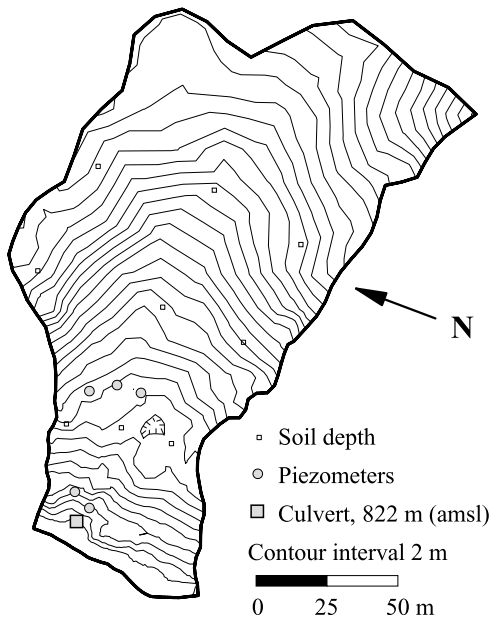


**Figure 2.** The C3 catchment topography with measurement locations.

intersected along its downstream boundary by a forest road, which is drained by a culvert. Mean annual precipitation at the H. J. Andrews Experimental Forest ranges from 2.30 m in lower elevations to 3.60 m along the highest ridges. The clay-rich upper and lower soil horizons are underlain by Miocene age volcanic and volcanoclastic bedrock. Figure 2 shows the convergent topography of the C3 catchment with measurement locations.

[12] The C3 database [Wemple, 1998; Dutton, 2000] includes measurements of topography, rainfall intensity, characteristics of the soil (thicknesses, saturated hydraulic

conductivity, porosity, and nonhysteretic capillary pressure relationships), and hydrologic response (observed time series of hydraulic head and discharge). Although some Dunne overland flow occurs at C3 (B. Wemple, personal communication, 2007) because of subsurface flow convergence, the humid climate, steep topography, and deep, permeable soils at C3 promote subsurface stormflow as the dominant mechanism (Figure 1). The C3 catchment was used to investigate the impacts of forest roads on slope stability [Dutton et al., 2005; Mirus et al., 2007]. The InHM simulated hydrologic response for the C3 base case was successful at capturing the observed nuances of both the integrated and distributed responses as described by Mirus et al. [2007].

**3.2. The CB Base Case Boundary Value Problem**

[13] The Coos Bay experimental catchment (CB) is located northeast of Coos Bay and North Bend in the Oregon Coast Range. A series of sprinkling experiments were conducted at CB during the early 1990s to investigate hydrologically driven landslide initiation. The unchanneled CB is less than 0.1 ha in area, is very steep (43°), and was clear-cut prior to the sprinkling experiments. Mean annual rainfall in North Bend is 1.6 m. The surface colluvium at CB is underlain by saprolite, weathered bedrock, and fractured sandstone. Figure 3 shows the steep topography of the CB catchment with measurement locations and the spatial variability in rainfall intensity and colluvium thickness.

[14] The CB database [Anderson et al., 1997a, 1997b; Montgomery et al., 1997; Torres et al., 1998; Ebel et al., 2007a] includes extensive measurements of topography, rainfall intensity, characteristics of the colluvium and underlying formations (geometry and thickness, saturated hydraulic conductivity, porosity, and hysteretic capillary pressure relationships), and hydrologic response (observed time series of soil water content, pressure head, discharge, and tracer

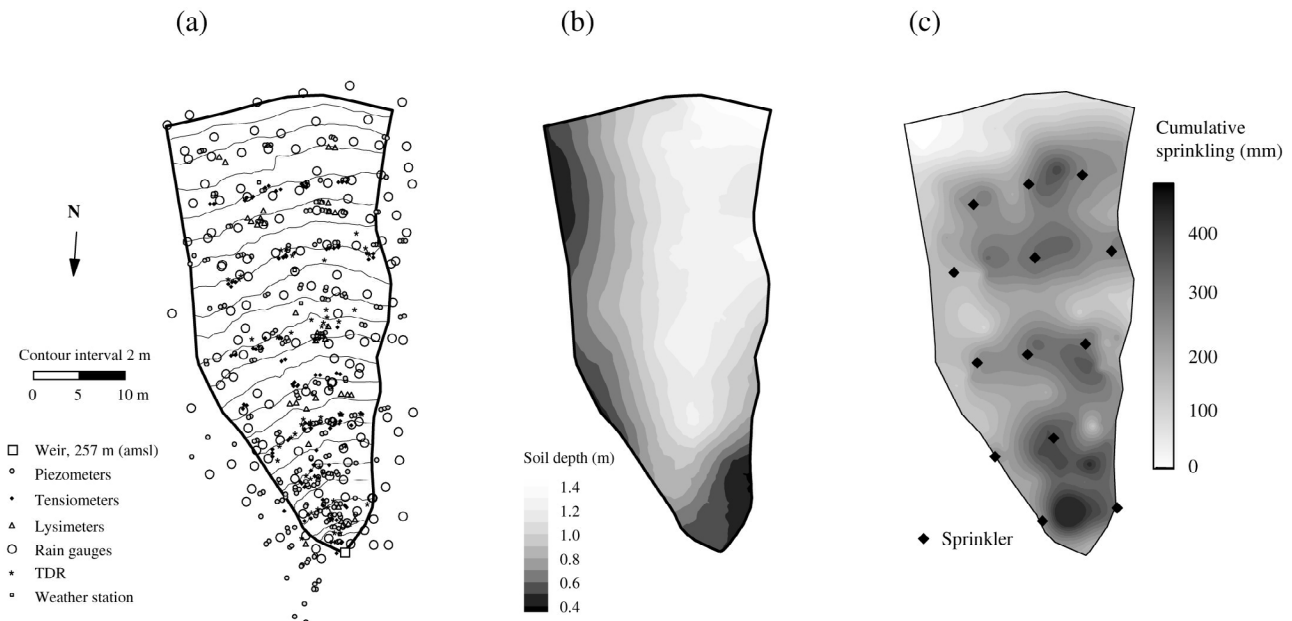


**Figure 3.** The CB catchment (a) topography with measurement locations, (b) spatial variability in soil depth, and (c) spatial variability in rainfall intensity.

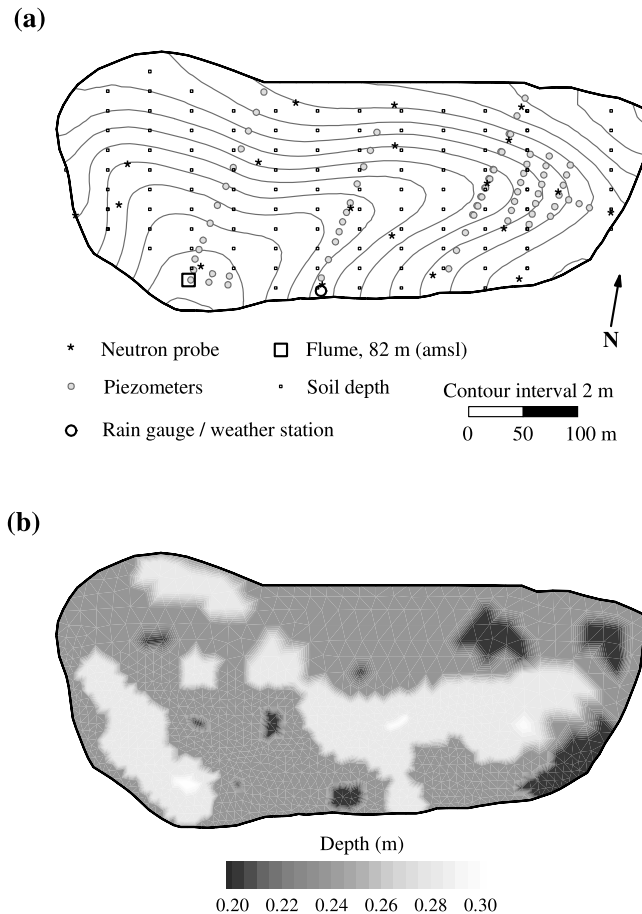


**Figure 4.** The TW catchment (a) topography with measurement locations and (b) spatial variability in soil depth.

concentrations). The highly permeable near surface, steep slopes, and humid climate favor subsurface stormflow as the dominant mechanism (Figure 1). The heavily instrumented and monitored CB has facilitated rigorous evaluation of the InHM base case boundary value problem as described by *Ebel et al.* [2007b].

### 3.3. The TW Base Case Boundary Value Problem

[15] The experimental catchment known as Tarrawarra (TW) is located in southeastern Australia. This well-managed rangeland catchment was heavily monitored in the mid-1990s to examine interactions between rainfall and evapotranspiration with runoff and soil moisture dynamics. The first-order TW is 10.5 ha in area, gently sloping ( $2^\circ$ ), and vegetated with grasses. Mean annual precipitation at TW is approximately 0.82 m. The soils across TW are silty and silty-clay loams, which overlay siltstone bedrock. Figure 4 shows the two convergent hollows and the gently sloping topography of TW with measurement locations and the spatial variability in topsoil thickness.

[16] The TW database [*Western and Grayson, 1998*] includes extensive measurements of topography, rainfall intensity, characteristics of the soil horizons (geometry and thickness, saturated hydraulic conductivity, porosity, and texture), and hydrologic response (observed time series of soil water content, pressure head, and discharge), as well as

characterization of the land cover and estimates of potential evapotranspiration. The climate and terrain at TW promote runoff response dominated by the Dunne mechanism (see Figure 1). The TW data set played a central role in the development of an exhaustive synthetic data set of a Tarrawarra-like hydrologic response, which successfully captures observations of both the integrated and distributed hydrologic responses as described by *Mirus et al.* [2009a].

### 3.4. The R5 Base Case Boundary Value Problem

[17] The experimental site known as R5 is located near Chickasha, Oklahoma. A well-managed rangeland catchment that was intensely monitored during the International Hydrologic Decade, R5 has a tremendous database. The first-order R5 is 9.6 ha in area, gently sloping ( $3^\circ$ ), and vegetated with native grasses. Mean annual rainfall at R5 is approximately 0.73 m. The silt loam soils are underlain by a heterogeneous mix of shale, siltstone, and sandstone of the Chickasha Formation. Figure 4 illustrates the gently sloping topography of the R5 catchment with measurement locations and the spatial variability in infiltration capacity.

[18] The R5 database [*Heppner and Loague, 2008*] includes extensive measurements of rainfall intensity, topography, characteristics of the soil horizons (thickness, infiltration capacity, porosity, and texture), and hydrologic response (observed time series of soil water content and discharge), as well as characterization of the vegetation and land cover and estimates of potential evapotranspiration. The climate, terrain, and soil hydraulic properties at R5 facilitate runoff by the Horton and Dunne mechanisms (see Figure 1). The R5 data set played a central role in the development and testing of InHM [*VanderKwaak and Loague, 2001; Loague et al., 2005; Heppner et al., 2007; Ebel et al., 2009*]. The R5 boundary value problem has evolved over the years, culminating in the base case scenario described by *Heppner et al.* [2007].

## 4. Methods: Investigations of Boundary Value Problem Complexity

[19] As illustrated by *Mirus et al.* [2007], *Ebel et al.* [2007b], *Mirus et al.* [2009a], and *Heppner et al.* [2007], successful parameterization and evaluation of InHM for the C3, CB, TW, and R5 base cases, respectively, relied on the availability of an extensive catchment-scale data set. However, the four data sets each include different amounts of detail (see Table 2), dictated by the objectives of the studies for which they were collected and a priori perceptions of the dominant processes. The degree of detail represented in each base case boundary value problem therefore varies, depending on the observational detail within the corresponding catchment-scale data set (see Figures 2–5). For example, data from 148 rain gauges were used to incorporate the spatially variable sprinkling into the CB base case boundary value problem, while the C3, TW, and R5 base cases each rely on individual rain gauges to assign spatially uniform rainfall rates (Table 2). Differences between the characteristics of the four base case scenarios, such as the spatial variability of rainfall (or lack thereof), prevent an even comparison of simulation results between different catchments.

[20] The relative impact on simulated process representation for each type of boundary value problem characteristic was investigated by simplifying each base case into a

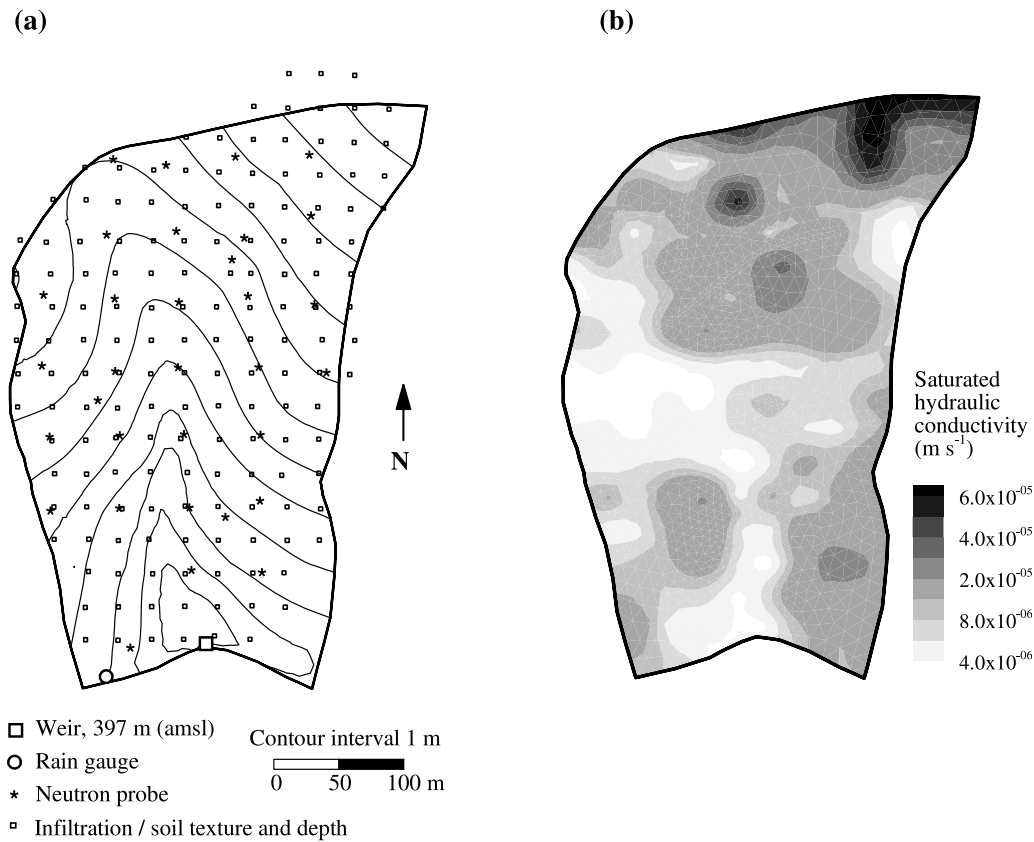


**Figure 5.** The R5 catchment (a) topography with measurement locations and (b) spatial variability in saturated hydraulic conductivity.

corresponding reduced case, such that the reduced cases for all four catchments share a common level of boundary value problem complexity. For example, reduced case simulation scenarios all apply spatially uniform rainfall rates. Table 3 summarizes the relevant differences between the four base case boundary value problems. Of the four catchment-scale data sets (Table 2), the C3 database supported the development of the simplest base case boundary value problem (Table 3). The C3 base case exemplifies the level of boundary value problem simplicity needed for the reduced cases developed in this study; therefore, the C3 base and reduced case parameterizations are identical. Relative to the complexity of the original base case boundary value problems, the simplifications presented are modest, and the

reduced case scenarios retain considerable information. Table 4 provides complete InHM parameterizations of the four reduced cases established for this study.

#### 4.1. Rainfall Events

[21] Evaluation of the conversion from the base to the reduced case scenarios employed one rainfall-runoff event from the observed records of each catchment. Rainfall events from the C3, TW, and R5 base case data sets were selected using the following criteria: (1) the rainfall event ranks among the largest for the catchment in terms of peak rainfall rate and total precipitation depth, (2) the event displays one of the largest observed runoff coefficients (i.e., ratio of total surface runoff to precipitation), (3) the

**Table 3.** Characteristics of the C3, TW, R5, and CB Base and Reduced Case Scenarios

Characteristic	Base Case Scenario				Reduced Case Scenarios C3, CB, TW, and R5
	C3	CB	TW	R5	
Rainfall, spatially variable	no	yes	no	no	no <sup>a</sup>
Hydraulic conductivity, spatially variable	no	no	no	yes	no <sup>b</sup>
Soil depth, spatially variable	no	yes	yes	no	no <sup>c</sup>
Evapotranspiration	no	no	yes <sup>d</sup>	yes <sup>d</sup>	no <sup>e</sup>
Water retention curve, hysteretic	no	yes	no	no	no <sup>f</sup>

<sup>a</sup>Spatially variable rainfall is replaced with uniform intensity equal to the mean value from three automated gauges [Ebel *et al.*, 2007a].

<sup>b</sup>Saturated hydraulic conductivity is equal to the geometric mean of the maximum and minimum values from the base case.

<sup>c</sup>Each soil layer with spatially variable thickness is replaced with a layer of uniform thickness equal to mean thickness of the base case.

<sup>d</sup>Depth-distributed evapotranspiration.

<sup>e</sup>Evapotranspiration is removed from all reduced case scenarios.

<sup>f</sup>Hysteretic water retention curve is replaced with the nonhysteretic wetting curve, as recommended by Ebel *et al.* [2010].

**Table 4.** Characteristics of the Four Reduced Case Boundary Value Problems<sup>a</sup>

Characteristic	C3	CB	TW	R5
<i>Finite Element Mesh</i>				
Number of nodes				
Surface	1,128	2,774	1,335	1,603
Subsurface	80,088	138,544	73,425	62,517
Space increments (m)				
Horizontal <sup>b</sup> ( $x, y$ )	0.7–20.0	0.4–2.3	4.0–15.0	8.8–22.0
Vertical <sup>c</sup> ( $z$ )				
Topsoil	0.05	0.10	0.02	0.05
Subsoil 1	0.15	na <sup>d</sup>	0.05–0.07	0.05
Subsoil 2	na <sup>d</sup>	0.02–0.19	na <sup>d</sup>	0.05–0.15
Bedrock	0.3–4.0	1.67	0.10–2.00	0.25
<i>Boundary Conditions<sup>e</sup></i>				
Surface				
Applied flux	PPT	PPT	PPT	PPT
Outlet	CD <sup>f</sup>	CD <sup>g</sup>	CD	RC <sup>h</sup>
Sides	IP	IP	IP	IP
Subsurface (faces)				
Up gradient	IP	IP	IP	IP
Down gradient	RS	RS	RF	RS
Sides	IP	IP	IP	IP
Base	IP	IP	RF	UG
<i>Subsurface Hydraulic Properties</i>				
Layer thickness (m)				
Topsoil	1.5	0.96	0.23	0.2
Subsoil 1	1.5	na <sup>d</sup>	1.0	0.2
Subsoil 2	na <sup>d</sup>	2.0	na <sup>d</sup>	1.4
Bedrock	100	53	20	5
Saturated hydraulic conductivity ( $\text{m s}^{-1}$ )				
Topsoil	$1.0 \times 10^{-3}$	$3.4 \times 10^{-4}$	$2.0 \times 10^{-6}$	$1.4 \times 10^{-5}$
Subsoil 1	$7.0 \times 10^{-4}$	na <sup>d</sup>	$2.0 \times 10^{-7}$	$4.3 \times 10^{-6}$
Subsoil 2	na <sup>d</sup>	$7.2 \times 10^{-5}$	na <sup>d</sup>	$4.3 \times 10^{-7}$
Bedrock	$1.0 \times 10^{-9}$	$5.0 \times 10^{-7}$	$2.0 \times 10^{-9}$	$4.5 \times 10^{-9}$
Characteristic curves <sup>i</sup>				
$\alpha$ ( $\text{m}^{-1}$ )				
Topsoil	2.0	35.0	4.0	1.3
Subsoil 1	2.0	na <sup>d</sup>	4.5	1.8
Subsoil 2	na <sup>d</sup>	4.3	na <sup>d</sup>	0.6
Bedrock	4.3	4.3	6.0	0.6
$\beta$				
Topsoil	1.4	3.0	2.5	1.7
Subsoil 1	1.4	na <sup>d</sup>	2.0	1.6
Subsoil 2	na <sup>d</sup>	1.3	na <sup>d</sup>	1.7
Bedrock	1.25	1.3	1.5	1.7
Residual water content ( $\text{m}^3 \text{m}^{-3}$ )				
Topsoil	0.15	0.16	0.14	0.09
Subsoil 1	0.15	na <sup>d</sup>	0.11	0.13
Subsoil 2	na <sup>d</sup>	0.01	na <sup>d</sup>	0.16
Bedrock	0.02	0.01	0.02	0.02
Porosity ( $\text{m}^3 \text{m}^{-3}$ )				
Topsoil	0.4	0.5	0.48	0.44
Subsoil 1	0.4	na <sup>d</sup>	0.38	0.48
Subsoil 2	na <sup>d</sup>	0.15	na <sup>d</sup>	0.41
Bedrock	0.2	0.12	0.2	0.3
Compressibility ( $\text{m}^2 \text{N}^{-1}$ )				
Topsoil	$1 \times 10^{-7}$	$1 \times 10^{-8}$	$1 \times 10^{-7}$	0
Subsoil 1	$1 \times 10^{-7}$	na <sup>d</sup>	$1 \times 10^{-7}$	0
Subsoil 2	na <sup>d</sup>	$1 \times 10^{-9}$	na <sup>d</sup>	0
Bedrock	$1 \times 10^{-9}$	$1 \times 10^{-9}$	$1 \times 10^{-9}$	0
<i>Surface Properties</i>				
Surface roughness <sup>j</sup>	0.35	0.35	0.35	0.10
Depression storage (m)	0.01	0.005	0.01	0.005
Mobile water depth (m)	0.0001	0.005	0.0001	0.0005
Surface coupling length <sup>k</sup> (m)	$1 \times 10^{-4}$	$1 \times 10^{-3}$	$1 \times 10^{-3}$	$1 \times 10^{-2}$

**Table 5.** Characteristics of the Individual Rainfall Events Selected for Illustrating the Impact of the Base Case Reductions

Catchment	Event	Start date	Total Depth (mm)	Maximum Intensity (mm h <sup>-1</sup> )	Time to Maximum Intensity (h)	Storm Duration (h)	Time Since Last Rain (days)
C3	event 1 <sup>a</sup>	27 Nov 1996	286	7.1	163	226	5
CB	experiment 3 <sup>b</sup>	27 May 1992	72	2.0	84	166	0.5
TW	event 6a <sup>c</sup>	29 Sep 1996	19	2.8	44	70	2
R5	event 68 <sup>d</sup>	29 Apr 1974	50	76.3	2	4	8

<sup>a</sup>Mirus et al. [2007].

<sup>b</sup>Ebel et al. [2007a].

<sup>c</sup>Mirus et al. [2009a].

<sup>d</sup>Heppner et al. [2007].

observed and simulated hydrographs for the event display a distinct cause and effect response, and (4) the initial conditions for the event are subject to no prior rainfall for at least 1 day. The data set used for developing the CB base case consists of three artificial sprinkling experiments [see Ebel et al., 2007a]; therefore, a different criterion was used to select the event. Experiment 3 was selected for this study because it includes the most observational detail of the three experiments. The characteristics of the selected rainfall and sprinkling events for the four catchments are given in Table 5.

#### 4.2. Initial Conditions

[22] Realistic and internally valid initial conditions for each simulation scenario were developed using warm-up simulations conducted with InHM. The initial conditions were designed to produce subsurface pressure head distributions and surface water depth patterns similar to those that developed prior to the corresponding event in the continuous simulations wherein the base case parameterizations were originally established [see Mirus et al., 2007; Ebel et al., 2007b; Mirus et al., 2009a; Heppner et al., 2007]. The initial condition for each warm-up simulation is a uniform water depth assigned to all surface nodes and total head values for subsurface nodes specified as a percentage of elevation at the surface. The warm-up simulations commence with a preliminary period of redistribution and drainage, followed by an applied rainfall flux (during which drainage continues), and concludes with a period of drainage only. When employing the warm-up simulation approach, it is not possible to develop identical initial conditions for different boundary value problems. However, the warm-up simulation protocol for the base and reduced case scenarios is the same for each catchment, as summarized in Table 6. Therefore, the impact of reduction in boundary value problem complexity for each

reduced case scenario is, by necessity, embedded in the warm-up simulation for that scenario.

### 5. Simulation Results

[23] Simulation results for the base and reduced case scenarios for C3, CB, TW, and R5 are shown in Figures 6–9. The integrated response is shown in terms of discharge hydrographs, whereas the distributed response is presented in terms of surface water depth snapshots at selected output times. Because the surface water depth patterns change through time, surface water depth is considered a surrogate for overland flow wherever it exceeds the mobile water depth of a given boundary value problem. Sections 5.1–5.4 describe the simulation results for each catchment, focusing on the impacts (integrated and distributed) of removing complexity from the individual boundary value problems (see Table 3).

#### 5.1. The C3 Reduced Case

[24] Since the InHM parameterization for the C3 base and reduced cases is identical, the simulated hydrologic response is the same for both scenarios. Discharge rises gradually as cumulative rainfall increases, then rises more rapidly as rainfall rates increase, approaching peak intensities (Figure 6, output time B). Peak discharge occurs approximately 1 day after peak rainfall intensity (Figure 6, output time C). Discharge begins to fall gradually as high-intensity rainfall tapers off and continues dropping well after the cessation of rainfall. Overall, discharge on the falling limb of the hydrograph decreases smoothly at roughly the average rate of increase on the rising limb and levels off more than 4 days after rainfall ceases (Figure 6, output time D).

[25] Exfiltration of subsurface stormflow along the roadcut dominates the integrated response, with only minor

#### Notes to Table 4:

<sup>a</sup>The values for gravitational acceleration, the density of water, and the dynamic viscosity of water were taken as 9.8 m<sup>2</sup> s<sup>-1</sup>, 1000 kg m<sup>-3</sup>, and 0.001138 kg m<sup>-1</sup> s<sup>-1</sup>, respectively.

<sup>b</sup>Maximum horizontal spacing.

<sup>c</sup>Range of vertical mesh spacing for each hydrogeologic unit, which increases with depth.

<sup>d</sup>No subsoil 1 at CB; no subsoil 2 at C3 or TW.

<sup>e</sup>Boundary conditions: PPT, precipitation; CD, critical depth; RC, rating curve; IP, impermeable; RS, regional sink; RF, radiation flux; UG, unity gradient.

<sup>f</sup>Culvert.

<sup>g</sup>Upper weir.

<sup>h</sup>V notch weir.

<sup>i</sup>Soil water content and unsaturated hydraulic conductivity as functions of pressure head represented by van Genuchten curve shape parameters [van Genuchten, 1980].

<sup>j</sup>Represented by Manning's *n* values.

<sup>k</sup>See VanderKwaak [1999] and Ebel et al. [2009].

**Table 6.** Characteristics of InHM Warm-up Simulations

Catchment	Initial Total Head <sup>a</sup> (%)	Initial Water Depth <sup>b</sup> (mm)	Total Simulation Duration (h)	Rainfall Characteristics		
				Start (h)	Stop (h)	Intensity (mm h <sup>-1</sup> )
C3	99.99	0.10	1839	920	1839	0.4 <sup>c</sup>
CB	99.00	0.01	42	0	42	1.8
TW	99.50	0.10	48	0	22	1.8
R5	83.30	1.00	52	0.3	42	18.0

<sup>a</sup>Total head values for subsurface nodes throughout domain assigned initial values equal to specified percentage of corresponding surface elevation.

<sup>b</sup>Uniform initial depth assigned throughout catchment.

<sup>c</sup>Mean intensity from variable precipitation rate [Mirus et al., 2007].

contributions from rainfall delivered to the continuously saturated road surface (Figure 6, output times A–D). The importance of the road in governing the integrated response is revealed by the gradual decrease in surface water depth along the roadcut after rainfall ceases, while the remainder of the catchment is dry at the surface (Figure 6, output time D). The Dunne mechanism occurs within the break in slope in the lower portion of the hollow, where the convergence of subsurface flow drives the water table to the surface (Figure 6, output time B). Even during peak discharge, Dunne overland flow remains localized within this small area before it infiltrates farther downslope and does not contribute directly to the integrated response (Figure 6,

output time C). The variable source area for Dunne overland flow dissipates shortly after rainfall ceases and before discharge recedes (Figure 6 output time D).

[26] Despite the spatially uniform soil depth, hydraulic properties, and rainfall intensity, as well as the absence of evapotranspiration and hysteretic water retention relationships in the C3 base and reduced case scenarios, the InHM simulation captures both the subsurface stormflow and Dunne overland flow mechanisms.

## 5.2. The CB Reduced Case Conversion

[27] The differences between the CB base and reduced cases include the spatial variability in soil depth and rainfall

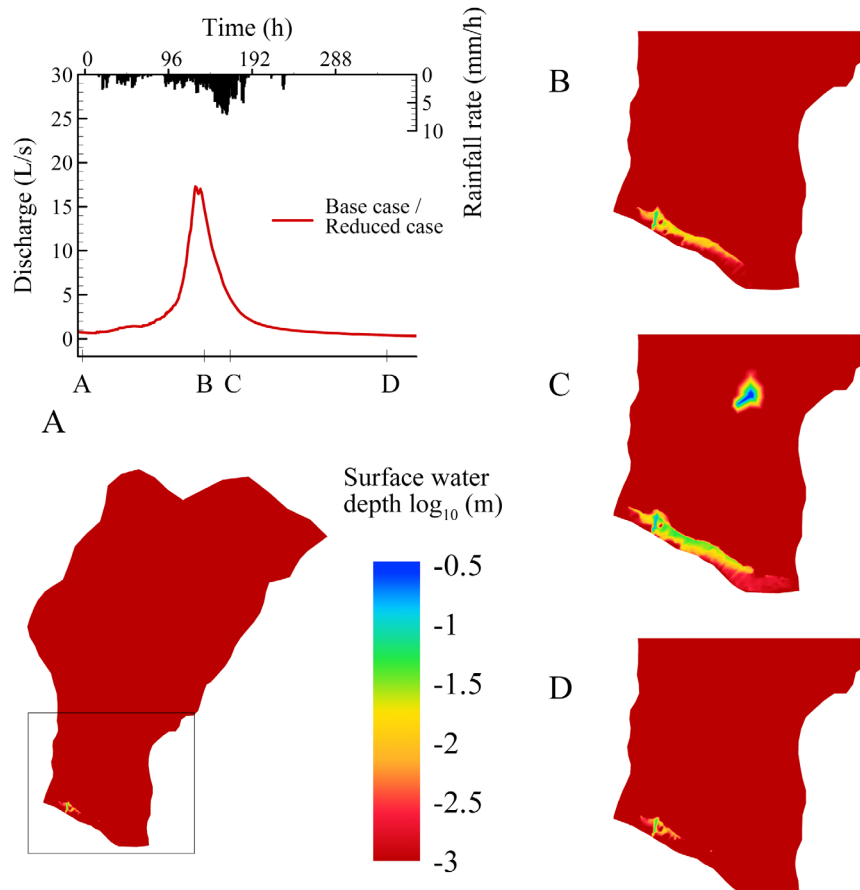


**Figure 6.** C3 base and reduced case simulated response for event 1 with hyetograph, hydrograph, and snapshots of the surface water depths for selected output times.

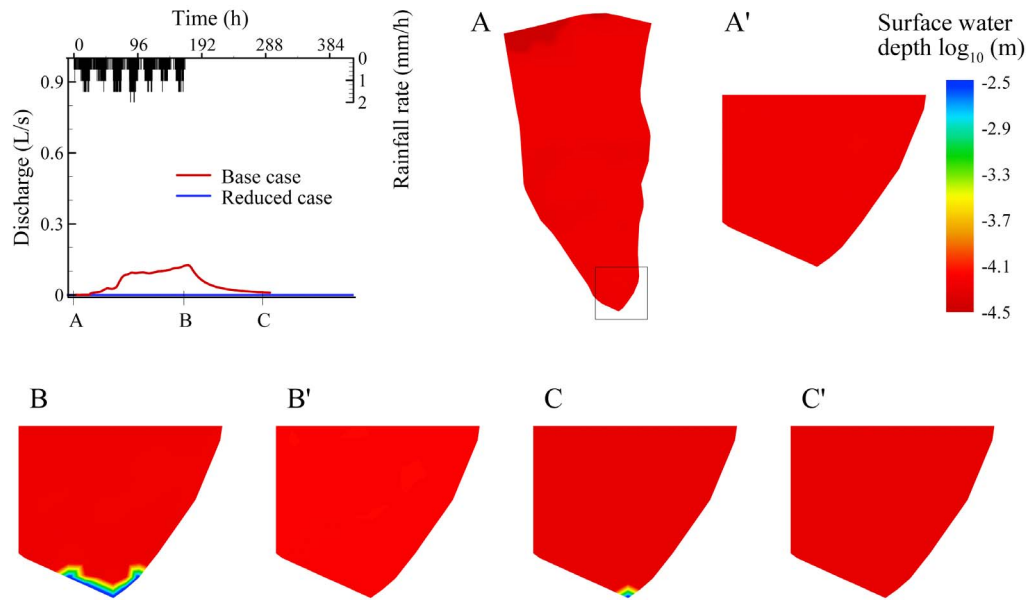


**Figure 7.** CB base and reduced case simulated responses for experiment 3 with hyetograph, hydrograph, and snapshots of the surface water depths for selected output times. Distributed snapshots for the reduced case are indicated with a prime.

intensity, as well as the hysteretic water retention relationships (Table 3). For the base case scenario, discharge rises gradually after about a day of steady sprinkling and then increases sharply after several more days of sprinkling before leveling off to a low, near-steady discharge for the remainder of the experiment. Peak discharge for the base case coincides with the cessation of the week-long sprinkling experiment (Figure 7, output time B). In contrast, the reduced case does not produce surface runoff for the entirety of the low-intensity sprinkling event. The down-gradient seepage face is generated for the base case because the CB weir and decreased thickness in the colluvium unit (Figure 3b) promote the exfiltration of subsurface stormflow. Exfiltration occurs only when rainfall intensities and total depth are sufficient to exceed leakage into the bedrock and lateral drainage via subsurface stormflow, thereby locally elevating the perched water table close to the surface just upslope of the weir. While the averaged uniform soil depth for the CB reduced case diminishes the conditions favoring seepage, the removal of spatially variable rainfall is the primary reason for the lack of surface runoff at the weir in the CB reduced case.

[28] The spatially variable rainfall intensities employed for the reduced case are based on the 148 manual gauges placed throughout the catchment (Table 2 and Figure 3a), whereas the spatially uniform rainfall intensities employed for the reduced case represent the mean rates captured by three automated rain gauges (Tables 3 and 5). The manual rain gauges were monitored roughly every 10 h, whereas the automated rain gauges measured every 10 min. This problem of a space-time trade-off [see *Loague*, 1991] is further complicated by comparison of the cumulative rainfall depth estimated for the base case (250 mm) and reduced case (72 mm). The difference between the automated and manual gage totals is the result of wind-driven undercatch of sprinkling because of the elevated automated gage heights [*Ebel et al.*, 2007a]. Although the automated rain gauges

provide high temporal resolution, analysis of the manual gauges leads to a more complete estimate of the total storm depth. The simulated impact of the lower rainfall total and the spatially uniform soil depth for the reduced case scenario is to limit the perched water table rise enough to prevent the development of a seepage face near the downstream boundary (Figure 7, output time B).

[29] The barely detectable variations in shallow water below the mobile water depth in the base case scenario (i.e., Figure 7, output time A) are due to the spatially variable rainfall intensities (Figure 3c), which are eliminated for the reduced case. The removal of hysteresis in the water retention curve has a minor impact on simulated runoff response as reported by *Ebel et al.* [2010]. In the CB reduced case conversion, only the simplified characterization of rainfall is sufficient to control the process threshold between entirely subsurface stormflow versus subsurface stormflow becoming surface runoff at the seepage face upslope of the weir.

### 5.3. The TW Reduced Case Conversion

[30] The differences between the TW base and reduced cases include the spatial variability in soil depth and consideration of evapotranspiration (Table 3). For both scenarios, discharge starts gradually, approximately 5 h after rainfall begins, and repeated bursts of low-intensity rainfall maintain a fluctuating, low discharge during the first 40 h. The elimination of evapotranspiration results in slightly greater discharge for the reduced case since drainage is the only other mechanism for removing water from the hillslopes between rainfall bursts (Figure 8, output time A). With sustained rainfall at moderately higher intensities, the hydrograph rises sharply for both scenarios (Figure 8, output time B) and after approximately 5 h reaches a peak discharge, which is slightly higher for the reduced case (Figure 8, output time C), again due to the absence of evapotranspiration. Discharge for both scenarios drops sharply with decreasing rainfall intensities

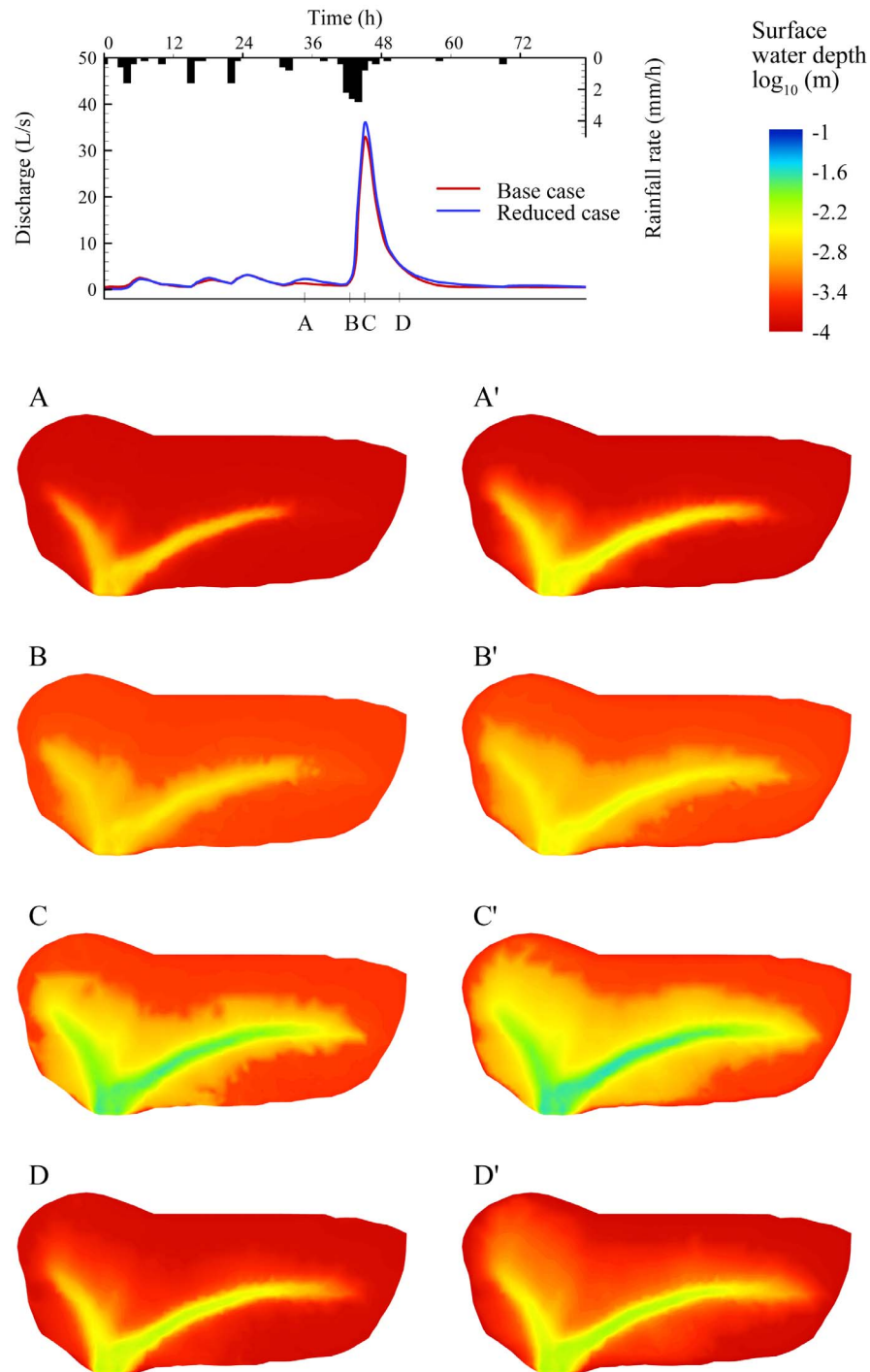


**Figure 8.** TW base and reduced case simulated responses for event 6a with hyetograph, hydrograph, and snapshots of the surface water depths for selected output times. Distributed snapshots for the reduced case are indicated with a prime.

and after 6 h of drainage begins to fall slowly, receding more gradually than the rising limb of the hydrograph, and leveling off approximately 20 h after peak discharge.

[31] For both the base and reduced case scenarios, surface saturation develops along the convergent topography early in the rainfall event (Figure 8, output time A). As cumulative rainfall increases, saturation extends throughout the catchment to maintain a large variable source area for Dunne overland flow (Figure 8, output times B and C). Fluctuations

in discharge and surface runoff patterns reflect the temporal variations in rainfall intensity, the impact of which is slightly higher for the reduced case where evapotranspiration is absent. Low rainfall intensities for event 6a (see Table 5) promote infiltration over runoff, thereby limiting the depth of overland flow. Exfiltration of subsurface flow in the convergent topography combined with the accumulation of Dunne overland flow contributes to steady runoff in the main hollow, which is slightly deeper and extends farther

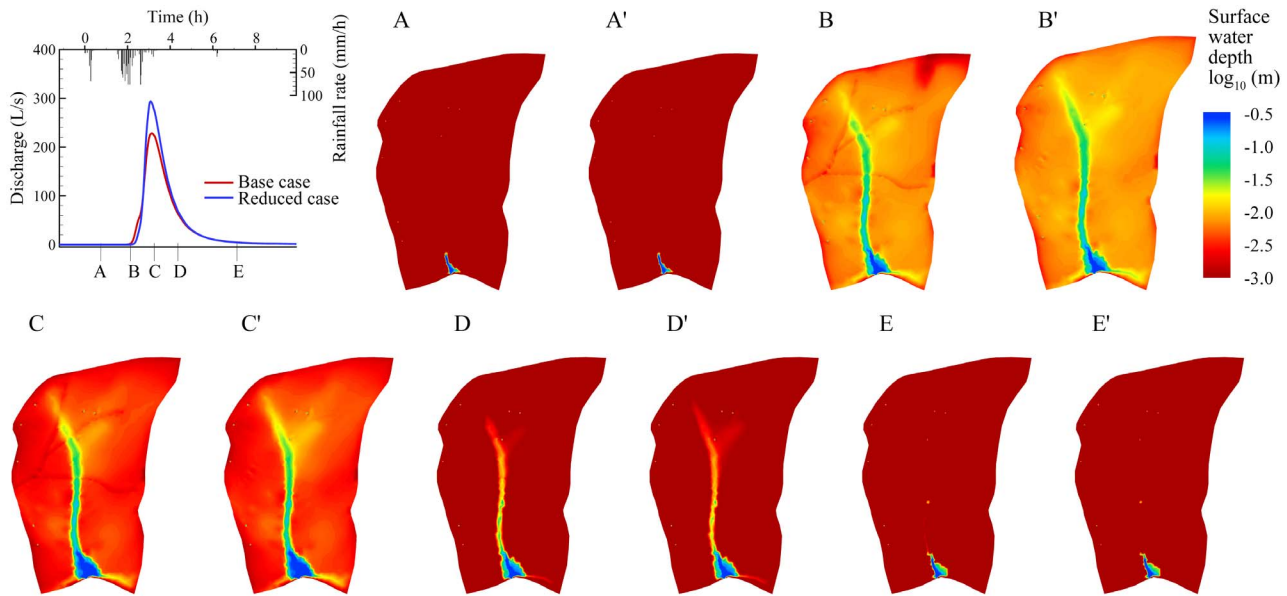


**Figure 9.** R5 base and reduced case simulated responses for event 68 with hyetograph, hydrograph, and snapshots of the surface water depths for selected output times. Distributed snapshots for the reduced case are indicated with a prime.

into the upper reaches of the catchment for the reduced case during peak discharge (Figure 8, output time C). After rainfall ceases, exfiltration sustains shallow overland flow within the main hollow for both the base and reduced case scenarios.

[32] Overall, the results illustrated in Figure 8 reveal that both scenarios for TW are similar, which is indicative of the moderate impact of evapotranspiration and the minor impact of spatially variable soil depth. In the TW reduced case conversion, the simplified representation of soil depth and removal of evapotranspiration did not control the process thresholds for Dunne overland flow.

#### 5.4. The R5 Reduced Case Conversion

[33] The differences between the R5 base and reduced cases include the spatial variability in infiltration capacity and consideration of evapotranspiration (Table 3). The simulation scenarios based on the R5 catchment employ topography that is a by-product of the construction of an artificial berm designed to focus runoff through the weir and a down-gradient pond. The characteristics of the weir and the topographic depression up gradient of the catchment outlet (see Figure 5a) affect the natural drainage of both surface and subsurface flows, which dictates the timing of the integrated response relative to the distributed response (Figure 9). The discharge reflects the depth of water above the weir, which does not correspond directly to the surface water depth patterns throughout the rest of the catchment (i.e., Figure 9, output times B and C). The lag between peak rainfall intensities and the onset of discharge at the weir for both the base and reduced case scenarios is therefore a result of this topographically enclosed depression, which must fill with standing water prior to the outflow of surface runoff at the downstream boundary (Figure 9, output time B).

[34] For the base case, the hydrograph begins to rise gradually with the final pulse of high-intensity rainfall

(Figure 9, output time B), and then discharge increases more rapidly as the rainfall intensities subside. In contrast, the onset of discharge for the reduced case is delayed until after rainfall intensities subside when the hydrograph rises sharply and continuously. The delay in discharge for the reduced case relative to the base case is due to the spatially uniform infiltration capacity, which eliminates several low-permeability patches, thereby delaying the onset of Horton overland flow to the periods of very high intensity rainfall. Conversely, the lack of high-permeability areas reduces overall infiltration, resulting in a higher peak discharge for the reduced case compared to the base case; the gradual decline on the receding limbs of the hydrographs is similar for both scenarios (Figure 9, output times D and E).

[35] Early in event 68, there is no overland flow throughout the catchment for either base or reduced case scenarios, and some standing water remains in the weir pond from the initial conditions warm-up simulation (Figure 9, output time A). Sustained rainfall at intensities greater than the infiltration capacity generates surface ponding; the Horton mechanism begins actively contributing to runoff once this ponding exceeds the mobile water depth and depression storage (see Table 4). For the base case, partial source areas of Horton overland flow develop first in the low-permeability regions within the weir pond and the surrounding topographically convergent areas (Figure 5b), then gradually spread to cover much of the catchment as rainfall intensities increase. For the reduced case, a spatially uniform infiltration capacity results in a uniform threshold for the Horton mechanism across the entire catchment ( $50 \text{ mm h}^{-1}$ ). In higher-permeability regions of the base case, near the drainage divides (Figure 5b), infiltration capacity exceeds rainfall intensities for the duration of event 68, which results in lower surface water depths relative to the reduced case (Figure 9, output times B and C).

[36] For both the base and reduced cases, Horton overland flow converges topographically, rapidly filling the weir

**Table 7.** Relative Impact of the Boundary Value Problem Characteristics on Simulated Hydrologic Response

Boundary Value Problem Characteristic	Hydrologic Response Impact		
	Discharge Hydrograph	Runoff Pattern	Runoff Generation Mechanism
Rainfall, spatially variable	moderate	moderate	none
Hydraulic conductivity, spatially variable	moderate	moderate	none
Soil depth, spatially variable	minor to moderate <sup>a</sup>	minor to moderate <sup>a</sup>	none
Evapotranspiration	none to moderate <sup>b</sup>	none to moderate <sup>b</sup>	none
Water retention curve, hysteretic	minor	none <sup>c</sup>	none

<sup>a</sup>Slope-dependent impact.

<sup>b</sup>Rainfall intensity-dependent impact.

<sup>c</sup>Runoff patterns are unaffected; impacts on subsurface pore pressure dynamics are discussed by *Ebel et al.* [2010].

pond, where continuous infiltration contributes to the rise and lateral expansion of a locally perched water table on the soil-bedrock interface. The intersection of this zone of perched saturation with the surface in topographically convergent areas produces the variable source area for Dunne overland flow (Figure 9, output times B–D). For both base and reduced cases, expansion and contraction of the variable source area is the result of temporal variations in the rainfall intensity. Outside the topographically convergent areas, overland flow remains slightly deeper for the reduced case as rainfall intensities decrease because of the lack of evapotranspiration, which causes drying in the near surface for the base case (Figure 9, output times C and D). After rainfall ceases, the perched water table recedes gradually at roughly the same rate for both cases, resulting in similar patterns of concentrated runoff within the topographically convergent areas (Figure 9, output times D and E).

[37] Overall, the results illustrated in Figure 9 reveal that eliminating both evapotranspiration and spatial variability in saturated hydraulic conductivity at the land surface has a notable impact on the integrated and distributed hydrologic responses. In terms of process representation, the Horton and Dunne mechanisms are both important contributors to runoff generation for the base and reduced case scenarios. In the R5 reduced case conversion the simplified representation of infiltration capacity and the removal of evapotranspiration were not sufficient to exceed the process thresholds for the occurrence of either Horton or Dunne overland flow.

## 6. Discussion

### 6.1. Impacts of Boundary Value Problem Complexity

[38] The results shown in Figures 6–9 reveal moderate changes in discharge and runoff patterns when simplifying to the reduced cases. Analysis of the simulation results indicates that the dominant runoff generation processes remain unchanged for each of the four base to reduced case conversions. Table 7 summarizes the relative impacts of the different boundary value problem characteristics on the integrated response, distributed response, and the overall runoff generation processes. The limited differences between the simulated hydrologic response for the base and reduced cases are not surprising given the relatively modest changes in boundary value problem complexity (Table 3) and the overwhelming information content retained in the reduced case scenarios (Table 4).

[39] Of the characteristics listed in Table 7, those observational details with the greatest influence on simulated runoff generation processes are the spatial variability in

three of the first-order controls on near-surface hydrologic response: (1) rainfall (CB), (2) hydraulic conductivity (R5), and (3) soil depth (CB and TW). These results echo previous studies focused on the hydrologic response impacts of spatial variability in rainfall intensity [e.g., *Ebel et al.*, 2007a], soil hydraulic properties [e.g., *Merz and Plate*, 1997], and depth to bedrock [e.g., *Tromp-van Meerveld and McDonnell*, 2006].

[40] The most obvious change in simulated response resulting from the conversions is the absence of the seepage face and surface runoff for the CB reduced case, which is primarily a result of the lower total rainfall depth. The lower total rainfall depth estimated using the mean from three automated tipping bucket rain gauges at CB (relative to the 148 manual rain gauges) highlights the challenges in obtaining reliable estimates of rainfall using point measurements [*Sieck et al.*, 2007]. Despite disparate estimates of total rainfall depth, the identical parameterizations of the hydrogeologic units for the CB base and reduced cases promotes subsurface stormflow through the high-permeability colluvium as the dominant mechanism for both cases. For scenarios with lower-permeability surface units than CB, the impact of the spatial variability in rainfall intensity (i.e., the barely detectable variations in shallow water depths for the CB base case) would likely have an important control on the Horton overland flow mechanism.

[41] The removal of spatially variable soil depth for the CB reduced case has a moderate, but lesser, impact on the integrated and distributed response than the rainfall characterization. In contrast to this moderate impact in the CB conversion, removing the relatively minor spatial variability in soil depth for TW has a negligible impact on the simulated hydrologic response in the reduced case. The discrepancy between the impacts of soil depth on the reduced case for CB compared to TW illustrates that the influence of soil depth on runoff generation is slope dependent and related to the dominant hydrologic response mechanism. The combination of soil depth, slope, and hydraulic properties affects the relative importance of Dunne overland flow and subsurface stormflow (see Figure 1). Soil depth influences unsaturated zone storage, which controls the Dunne mechanism. Slope and hydraulic conductivity dictate the rate at which the near-surface hydrogeologic units drain, which controls subsurface stormflow. The initial conditions warm-up simulation protocol employed for CB and TW were similar (Table 6), but the lower slope at TW (Table 1) results in slower drainage, which limits the importance of soil depth for the TW reduced case conversion. Spatial variations in soil depth influence the

occurrence of overland flow when drainage rates are high (e.g., CB), and the initial unsaturated storage conditions exert a stronger control on overland flow when drainage rates are slow (e.g., TW). The topographic controls on the threshold between subsurface stormflow and Dunne overland flow are also illustrated by the C3 reduced case, where subsurface stormflow dominates and Dunne overland flow occurs only within the break in slope (Figure 5). These examples suggest that detailed characterization of soil depth is more important where slopes are steep and that characterizing the initial conditions is more important on gentler slopes.

[42] Another substantial change in simulated response highlighted by the reduction of the base cases is the increased contribution of the Horton mechanism in the R5 reduced case. Comparison of the R5 base and reduced cases demonstrates that for the given rainfall event, the development of partial source areas for Horton overland flow are sensitive to order-of-magnitude variations in saturated hydraulic conductivity at the surface. However, because variations in saturated hydraulic conductivity do not strongly affect unsaturated zone storage dynamics for the gently sloping R5 topography (Figure 5), the contributions of Dunne overland flow to the integrated and distributed response remain largely unaffected by the base case reduction. Despite substantial temporal variations in rainfall intensity for R5 event 68, the average saturated hydraulic conductivity value employed for the R5 reduced case results in a reasonable representation of the base case hydrologic response processes. Although the R5 reduced case employs homogenous topsoil saturated hydraulic conductivity, the average uniform value was selected on the basis of information from 247 measurements. A single measurement of infiltration capacity is unlikely to provide a reasonable estimate for adequate simulated process representation of Horton overland flow.

[43] The exclusion of evapotranspiration has a variable impact on the simulated hydrologic response, displaying a moderate impact on the base to reduced case conversion for TW and a relatively minor impact for R5. The variability between the impacts for the TW and R5 base to reduced case conversions is due to the difference in the relative magnitude between potential evapotranspiration and rainfall characteristics for the two events. R5 event 68 is a short, high-intensity storm (Table 5), where the primary influence of evapotranspiration is on the initial infiltration capacity, which has a negligible impact on the onset of Horton overland flow because of the low ratio of topsoil saturated hydraulic conductivity to rainfall intensity. TW event 6a is a long, low-intensity storm (Table 5), where the primary influence of evapotranspiration is on increasing the available unsaturated zone storage between bursts of rainfall, which has a notable impact on the onset of Dunne overland flow. These unsaturated zone dynamics also explain why evapotranspiration has a greater impact than the spatial variability in soil depth on the TW base case reduction. Although evapotranspiration was not considered in the development of the C3 and CB base cases, nonhysteretic and hysteretic water retention curves were measured at the two catchments, respectively. These characteristic curves also impact the unsaturated zone storage dynamics between rainfall events. Whereas the hysteretic water retention curve influences the timing of the rising and falling limb of the hydrograph, it does not impact the dominance of subsurface stormflow for the relatively uniform experiment 3 sprinkling intensities at CB (Figure 7).

[44] Overall, examination of the simulation results from the base and reduced cases provides some insights into the utility of different types of observational detail for different environmental conditions and runoff generation mechanisms. In particular, the C3 scenario(s) demonstrate that the measurements of integrated response (i.e., total discharge) do not alone capture all the important processes. The C3, CB, TW, and R5 scenarios collectively demonstrate that some measure of the distributed water table response within topographically convergent areas (e.g., piezometer) is needed to identify the onset of the Dunne overland flow mechanism. The CB scenarios demonstrate that for very steep catchments, dominated by subsurface stormflow, accurate characterization of the average intensity and total rainfall depth are crucial for identifying the thresholds between subsurface stormflow and seepage that produces surface runoff. This suggests that the spatial extent of channel networks in subsurface stormflow-dominated systems is highly sensitive to the total depth of individual storms and the average rainfall intensity relative to the percolation leaking into the underlying unsaturated bedrock. The TW scenarios demonstrate that magnitudes of both rainfall intensity and evapotranspiration are important for quantifying the discharge and variable source area dynamics. The R5 scenarios demonstrate that a representative value of topsoil saturated hydraulic conductivity, in combination with accurate rainfall intensity measurements, is needed to identify the Horton overland flow mechanism. The C3, CB, TW, and R5 scenarios collectively demonstrate that the importance of unsaturated zone dynamics on different runoff generation mechanisms can vary on the basis of topography.

## 6.2. Strengths, Limitations, and Uncertainty

[45] The simulation results in Figures 6–9 demonstrate the capability of comprehensive physics-based models for examining distributed hydrologic response at high spatial and temporal resolutions. Using the high-resolution distributed response for the base case reductions, we confront one of the many challenges associated with applying distributed physics-based models across different environmental conditions: the variations between catchment-scale data sets available for model parameterization and evaluation. The problem of incommensurability [Beven, 1989] remains another major challenge to model parameterization and evaluation. Whereas field measurements of hydrologic state variables are often based on a support volume of several cubic centimeters, the sizes of model elements to which parameter values must be assigned in hydrologic models are typically on the order of a few cubic meters. Attempts to overcome this limitation are often based upon effective parameter values that compensate for sub-grid-scale heterogeneities and can be applied uniformly to different hydrogeologic units of a given model boundary value problem [Vereecken *et al.*, 2007]. This type of simplified conceptual model of heterogeneity can lead to mixed results for simulating observed moisture dynamics in soils with different degrees of pedogenic development and soil structure [Mirus *et al.*, 2009b]. The relatively minimal changes in the base case reductions presented in this study suggest that at the catchment scale, effective parameter values can provide a useful approach for employing a sophisticated physics-based model to examine the fundamental controls on runoff generation.

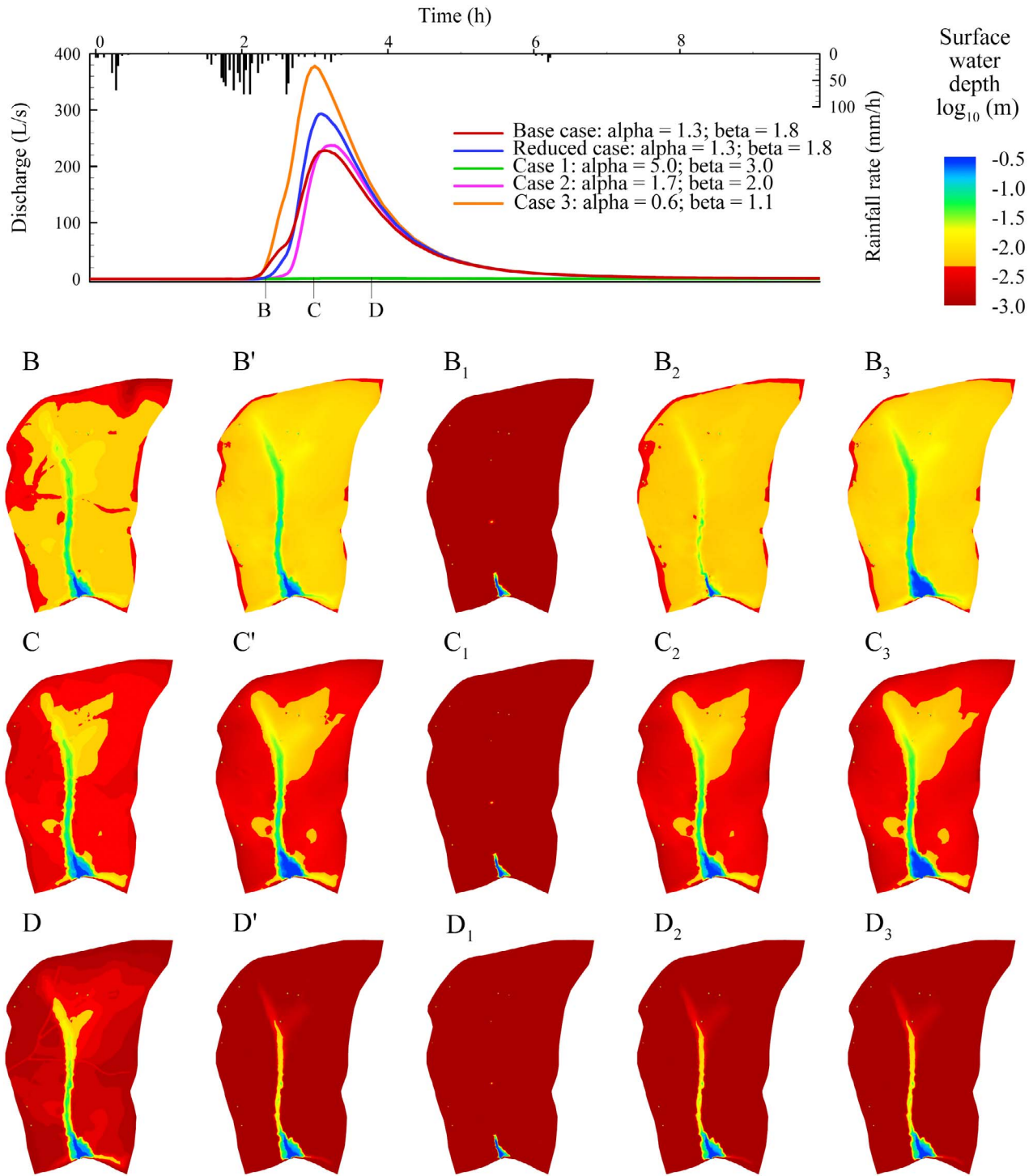


**Figure 10.** Simulated hydrologic response for R5 event 68 for the base case, reduced case (indicated by a prime), and cases 1, 2, and 3 with perturbed values of the *van Genuchten* [1980] parameters  $\alpha$  and  $\beta$ .

[46] A significant advantage of physics-based simulation related to data availability is that realistic parameter values can be independently constrained by direct measurements. These physical constraints on model parameterization facilitate a direct comparison between the sensitivity of simulated hydrologic response and simplifications in boundary value problem complexity with other sources of measurement uncertainty. To place the impact of the base case reductions

presented in this study in the broader context of other parameterizations of InHM, we present alternative simulation scenarios developed through perturbations of the R5 reduced case boundary value problem. The R5 boundary value problem was selected because the base case reduction results in a notable change in simulated hydrologic response relative to the other cases and exhibits both Horton and Dunne overland flow mechanisms. Figure 10 shows simulation

results for the R5 base and reduced cases compared to three cases where the *van Genuchten* [1980] parameters  $\alpha$  and  $\beta$  are perturbed. The perturbations represent modest changes in characteristic curve shapes that are well within the physically reasonable limits defined by the four boundary value problems described in Table 4. Examination of Figure 10 reveals that despite these minor changes, the impact on runoff response for the R5 rainfall event 68 (Table 5) is substantial compared to the impact of the base case reductions. In case 1, the characteristic curve sufficiently changes the unsaturated storage dynamics to prevent the occurrence of overland flow entirely. Case 2 illustrates that fractional changes in  $\alpha$  and  $\beta$  have a comparable impact on hydrologic response to the base case reduction. In case 3 the characteristic curves are sufficiently perturbed to increase both the Dunne and Horton overland flow response.

[47] The previous analyses have established the hydrologic realism of the individual base cases [VanderKwaak and Loague, 2001; Loague et al., 2005; Ebel and Loague, 2006; Mirus et al., 2007; Ebel et al., 2007a, 2007b, 2008; Heppner et al., 2007; Mirus et al., 2009a], but the complexity of each boundary value problem reflects the different types of information used in model parameterization and performance evaluation (see Table 2). When establishing the original base case boundary value problems, a few piezometers at R5 would have been useful at the expense of several of the 247 of infiltration experiments (see Table 2). The differences in observational detail expressed in the four boundary value problems was an impediment to cross comparison of simulation results, which provided the motivation for developing the reduced cases presented herein.

[48] The sensitivity of simulated hydrologic response to, for example, saturated hydraulic conductivity is well understood for individual places or scenarios [e.g., Loague, 1988; Binley et al., 1989a, 1989b; VanderKwaak and Loague, 2001]. In contrast, comparing the sensitivity of simulated runoff response to changes in hydraulic conductivity for the R5 and TW base cases is an insurmountable task when the soil depth for R5 is uniform and the hydraulic conductivity is spatially variable and vice versa for TW. The three additional cases in Figure 10 merely scratch the surface in demonstrating the potential utility of the generic reduced case scenarios for further concept development. With the same level of boundary value problem complexity, the reduced case boundary value problems can facilitate a cross comparison of the type of sensitivity analysis presented in Figure 10 within a physically realistic parameter space. Future work should explore the relative controls on runoff generation across the environmental conditions illustrated in Figure 1 by systematically perturbing the parameters listed in Table 4 for each of four reduced case boundary value problems.

## 7. Summary: Establishing a Baseline for Concept Development Simulations

[49] This work begins to consider how the disparities between catchment-scale data sets impact boundary value problem complexity for a comprehensive physics-based model and evaluates the corresponding influence on simulated hydrologic response. One important conclusion demonstrated by the reduced scenarios is that the sensitivity of simulations to the removal of heterogeneity differs depending on the environmental conditions (i.e., climate and topogra-

phy). The four base case reductions presented here support the hypothesis that the removal of the differing levels of observational detail does not fundamentally alter the simulated runoff generation processes. Further simplifications to the four reduced cases are possible but are beyond the scope of this work, which focuses on generalized surface runoff patterns and process representation in first-order catchments for individual events. The implications of this work should not be extrapolated beyond these areas without further investigation. For example, simulation-based investigations of soil water–plant dynamics or contaminant transport should obviously include explicit consideration of evapotranspiration and heterogeneity in hydraulic conductivity, respectively. Unlike the base cases, the reduced case scenarios are not intended to emulate real systems, but rather to represent fundamental response types. Because their parameterizations are physically realistic, the simulated response for each reduced case scenario represents one possible set of dominant runoff generation processes that may occur at different times or places within real systems.

[50] The four reduced case scenarios establish a baseline level of boundary value problem complexity for further concept development simulations aimed at quantitatively characterizing the controls on runoff generation processes. The common level of complexity shared by the four reduced cases provides an unbiased starting point for cross comparison between simulations over a range of environmental conditions where different mechanisms may dominate (Figure 1). Improved quantitative understanding of the controls on the runoff generation mechanisms illustrated in Figure 1 is necessary for the appropriate selection of simpler, single-process models for applications in the decision-making and management arena. The reduced cases demonstrate that physics-based distributed models could be employed to improve fundamental understanding of controls on runoff generation processes without overly extensive representation of heterogeneities observed in the field. Furthermore, concept development simulations similar to those presented herein can be useful for determining data worth and designing networks for long-term monitoring of hydrologic response.

[51] **Acknowledgments.** This work was supported in part by the Stanford UPS Endowment Fund, a Stanford Graduate Fellowship, and NSF grant EAR-0537410. Thanks are owed to Steve Burges and Bob Street for their thoughtful comments on a prior version of this paper. We also appreciate the continued support of our long-term colleague, Joel VanderKwaak.

## References

- Anderson, S. P., W. E. Dietrich, R. Torres, D. R. Montgomery, and K. Loague (1997a), Concentration–discharge relationships in a steep unchanneled catchment, *Water Resour. Res.*, **33**, 211–225, doi:10.1029/96WR02715.
- Anderson, S. P., W. E. Dietrich, D. R. Montgomery, R. Torres, M. E. Conrad, and K. Loague (1997b), Subsurface flow paths in a steep unchanneled catchment, *Water Resour. Res.*, **33**, 2637–2653, doi:10.1029/97WR02595.
- Beven, K. J. (1989), Changing ideas in hydrology—The case of physically based models, *J. Hydrol.*, **105**, 157–172, doi:10.1016/0022-1694(89)90101-7.
- Binley, A. M., J. Elgy, and K. J. Beven (1989a), A physically based model of heterogeneous hillslopes: 1. Runoff production, *Water Resour. Res.*, **25**, 1219–1226, doi:10.1029/WR025i006p01219.
- Binley, A. M., K. J. Beven, and J. Elgy (1989b), A physically based model of heterogeneous hillslopes: 2. Effective hydraulic conductivities, *Water Resour. Res.*, **25**, 1227–1233, doi:10.1029/WR025i006p01227.

- Dunne, T. (1978), Field studies of hillslope flow processes, in *Hillslope Hydrology*, edited by M. J. Kirkby, pp. 227–293, John Wiley, New York.
- Dunne, T., and R. D. Black (1970a), An experimental investigation of runoff production in permeable soils, *Water Resour. Res.*, *6*, 478–490, doi:10.1029/WR006i002p00478.
- Dunne, T., and R. D. Black (1970b), Partial area contributions to storm runoff in a small New England watershed, *Water Resour. Res.*, *6*, 1296–1311, doi:10.1029/WR006i005p01296.
- Dutton, A. L. (2000), Process-based simulations of near-surface hydrologic response for a forested upland catchment: The impact of a road, 151 pp., M.S. thesis, Stanford Univ., Stanford, Calif.
- Dutton, A. L., K. Loague, and B. C. Wemple (2005), Simulated effect of a forest road on near-surface hydrologic response and slope stability, *Earth Surf. Processes Landforms*, *30*, 325–338, doi:10.1002/esp.1144.
- Ebel, B. A., and K. Loague (2006), Physics-based hydrologic response simulation: Seeing through the fog of equifinality, *Hydrol. Processes*, *20*, 2887–2900, doi:10.1002/hyp.6388.
- Ebel, B. A., and K. Loague (2008), Rapid simulated hydrologic response within the variably saturated near surface, *Hydrol. Processes*, *22*, 464–471, doi:10.1002/hyp.6926.
- Ebel, B. A., K. Loague, W. E. Dietrich, D. R. Montgomery, R. Torres, S. P. Anderson, and T. W. Giambelluca (2007a), Near-surface hydrologic response for a steep, unchanneled catchment near Coos Bay, Oregon: 1. Sprinkling experiments, *Am. J. Sci.*, *307*, 678–708, doi:10.2475/04.2007.02.
- Ebel, B. A., K. Loague, J. E. VanderKwaak, W. E. Dietrich, D. R. Montgomery, R. Torres, and S. P. Anderson (2007b), Near-surface hydrologic response for a steep, unchanneled catchment near Coos Bay, Oregon: 2. Physics-based simulations, *Am. J. Sci.*, *307*, 709–748, doi:10.2475/04.2007.03.
- Ebel, B. A., K. Loague, D. R. Montgomery, and W. E. Dietrich (2008), Physics-based continuous simulation of long-term near-surface hydrologic response for the Coos Bay experimental catchment, *Water Resour. Res.*, *44*, W07417, doi:10.1029/2007WR006442.
- Ebel, B. A., B. B. Mirus, C. S. Heppner, J. E. VanderKwaak, and K. Loague (2009), First-order exchange coefficient coupling for simulating surface water-groundwater interactions: Parameter sensitivity and consistency with a physics-based approach, *Hydrol. Processes*, *23*, 1949–1959, doi:10.1002/hyp.7279.
- Ebel, B. A., K. Loague, and R. I. Borja, (2010), The impacts of hysteresis on variably saturated hydrologic response and slope failure, *Environ. Earth Sci.*, *61*, 1215–1225, doi:10.1007/s12665-009-0445-2.
- Freeze, R. A., and J. A. Cherry (1979), *Groundwater*, Prentice Hall, Englewood Cliffs, N. J.
- Freeze, R. A., and R. L. Harlan (1969), Blueprint for a physically based digitally simulated, hydrologic response model, *J. Hydrol.*, *9*, 237–258, doi:10.1016/0022-1694(69)90020-1.
- Heppner, C. S., and K. Loague (2008), Characterizing long-term hydrologic-response and sediment-transport for the R-5 catchment, *J. Environ. Qual.*, *37*, 2181–2191, doi:10.2134/jeq2007.0548.
- Heppner, C. S., K. Loague, and J. E. VanderKwaak (2007), Long-term InHM simulations of hydrologic response and sediment transport for the R-5 catchment, *Earth Surf. Processes Landforms*, *32*, 1273–1292, doi:10.1002/esp.1474.
- Hewlett, J. D., and A. R. Hibbert (1963), Moisture and energy conditions within a sloping soil mass during drainage, *J. Geophys. Res.*, *68*, 1081–1087, doi:10.1029/JZ068i004p01081.
- Horton, R. E. (1945), Erosional development of streams and their drainage basins; hydrophysical approach to quantitative morphology, *Geol. Soc. Am. Bull.*, *56*, 275–370, doi:10.1130/0016-7606(1945)56[275:EDOSAT]2.0.CO;2.
- Ivanov, V. Y., E. R. Vivoni, R. L. Bras, and D. Entekhabi (2004), Catchment hydrologic response with a fully distributed triangulated irregular network model, *Water Resour. Res.*, *40*, W11102, doi:10.1029/2004WR003218.
- Jones, J. P., E. A. Sudicky, and R. G. McLaren (2008), Application of a fully integrated surface subsurface flow model at the watershed-scale: A case study, *Water Resour. Res.*, *44*, W03407, doi:10.1029/2006WR005603.
- Kampf, S. K., and S. J. Burges (2007), A framework for classifying and comparing distributed hillslope and catchment hydrologic models, *Water Resour. Res.*, *43*, W05423, doi:10.1029/2006WR005370.
- Kollet, S. J., and R. M. Maxwell (2006), Integrated surface-groundwater flow modeling: A free-surface overland flow boundary condition in a parallel groundwater flow model, *Adv. Water Resour.*, *29*, 945–958, doi:10.1016/j.advwatres.2005.08.006.
- Kollet, S. J., and R. M. Maxwell (2008), Capturing the influence of groundwater dynamics on land surface processes using an integrated, distributed watershed model, *Water Resour. Res.*, *44*, W02402, doi:10.1029/2007WR006004.
- Li, Q., A. J. A. Unger, E. A. Sudicky, D. Kassenar, E. J. Wexler, and S. Shikaze (2008), Simulating the multi-seasonal response of a large-scale watershed with a 3D physically based hydrologic model, *J. Hydrol.*, *357*, 317–336, doi:10.1016/j.jhydrol.2008.05.024.
- Loague, K. (1986), An assessment of rainfall-runoff modeling methodology, Ph.D. dissertation, 299 pp., Univ. of B. C., Vancouver, Canada.
- Loague, K. (1988), Impact of rainfall and soil hydraulic property information on runoff predictions at the hillslope scale, *Water Resour. Res.*, *24*, 1501–1510, doi:10.1029/WR024i009p01501.
- Loague, K. (1991), Space-time tradeoffs across the hydrologic data sets of competing rainfall-runoff models: A preliminary analysis, *Water Resour. Bull.*, *27*, 781–789.
- Loague, K. (1992), Impact of overland flow plane characterization on event simulations with a quasi-physically based rainfall-runoff model, *Water Resour. Res.*, *28*, 2541–2545, doi:10.1029/92WR01309.
- Loague, K., and J. E. VanderKwaak (2004), Physics-based hydrologic response simulation: Platinum bridge, 1958 Edsel, or useful tool, *Hydrol. Processes*, *18*, 2949–2956, doi:10.1002/hyp.5737.
- Loague, K., C. S. Heppner, R. H. Abrams, J. E. VanderKwaak, A. E. Carr, and B. A. Ebel (2005), Further testing of the Integrated Hydrology Model (InHM): Event-based simulations for a small rangeland catchment located near Chickasha, Oklahoma, *Hydrol. Processes*, *19*, 1373–1398.
- Loague, K., C. S. Heppner, B. B. Mirus, B. A. Ebel, Q. Ran, A. E. Carr, S. H. BeVelle, and J. E. VanderKwaak (2006), Physics-based hydrologic-response simulation: Foundation for hydroecology and hydrogeomorphology, *Hydrol. Processes*, *20*, 1231–1237, doi:10.1002/hyp.6179.
- Loague, K., C. S. Heppner, B. A. Ebel, and J. E. VanderKwaak (2010), The Quixotic search for a comprehensive understanding of hydrologic response at the surface: Horton, Dunne, Dunton, and the role of concept-development simulations, *Hydrol. Processes*, *24*, 2499–2505, doi:10.1002/hyp.7834.
- McDonnell, J. J., et al. (2007), Moving beyond heterogeneity and process complexity: A new vision for watershed hydrology, *Water Resour. Res.*, *43*, W07301, doi:10.1029/2006WR005467.
- Merz, B., and E. J. Plate (1997), An analysis of the effects of spatial variability of soil and soil moisture on runoff, *Water Resour. Res.*, *33*, 2909–2922, doi:10.1029/97WR02204.
- Mirus, B. B., B. A. Ebel, K. Loague, and B. C. Wemple (2007), Simulated effect of a forest road on near-surface hydrologic response: Redux, *Earth Surf. Processes Landforms*, *32*, 126–142, doi:10.1002/esp.1387.
- Mirus, B. B., K. Loague, J. E. VanderKwaak, S. Kampf, and S. J. Burges (2009a), A hypothetical reality of Tarrawarra-like hydrologic response, *Hydrol. Processes*, *23*, 1093–1103, doi:10.1002/hyp.7241.
- Mirus, B. B., K. Perkins, J. R. Nimmo, and K. Singha (2009b), Hydrologic characterization of desert soils with varying degrees of pedogenesis: II. Inverse modeling for effective properties, *Vadose Zone J.*, *8*, 496–509, doi:10.2136/vzj2008.0051.
- Montgomery, D. R., W. E. Dietrich, R. Torres, S. P. Anderson, J. T. Heffner, and K. Loague (1997), Hydrologic response of a steep unchanneled valley to natural and applied rainfall, *Water Resour. Res.*, *33*, 91–109, doi:10.1029/96WR02985.
- Morita, M., and B.-C. Yen (2002), Modeling of conjunctive two-dimensional surface-three-dimensional subsurface flows, *J. Hydraul. Eng.*, *128*, 184–200, doi:10.1061/(ASCE)0733-9429(2002)128:2(184).
- Panday, S., and P. S. Huyakorn (2004), A fully coupled physically-based spatially-distributed model for evaluating surface/subsurface flow, *Adv. Water Resour.*, *27*, 361–382, doi:10.1016/j.advwatres.2004.02.016.
- Qu, Y., and C. J. Duffy (2007), A semidiscrete finite volume formulation for multiprocess watershed simulation, *Water Resour. Res.*, *43*, W08419, doi:10.1029/2006WR005752.
- Refsgaard, J. C. (2000), A formal approach to calibration and validation of models using spatial data, in *Spatial Patterns in Catchment Hydrology: Observations and Modelling*, edited by R. B. Grayson and G. Blöschl, pp. 355–367, Cambridge Univ. Press, Cambridge, U. K.
- Sieck, L. C., S. J. Burges, and M. Steiner (2007), Challenges in obtaining reliable measurements of point rainfall, *Water Resour. Res.*, *43*, W01420, doi:10.1029/2005WR004519.
- Therrien, R., R. G. McLaren, E. A. Sudicky, and S. M. Panday (2004), HydroGeoSphere: A three-dimensional numerical model describing fully integrated subsurface and surface flow and solute transport, user's guide, Groundwater Simul. Group, Univ. of Waterloo, Waterloo, Ont., Canada.
- Torres, R., W. E. Dietrich, D. R. Montgomery, S. P. Anderson, and K. Loague (1998), Unsaturated zone flow processes and the hydrologic response of a steep, unchanneled catchment, *Water Resour. Res.*, *34*, 1865–1879, doi:10.1029/98WR01140.

- Tromp-van Meerveld, H. J., and J. J. McDonnell (2006), Threshold relations in subsurface stormflow: 2. The fill and spill hypothesis, *Water Resour. Res.*, *42*, W02411, doi:10.1029/2004WR003800.
- van Genuchten, M. T. (1980), A closed-form equation for predicting the hydraulic conductivity of unsaturated soils, *Soil Sci. Soc. Am. J.*, *44*, 892–898, doi:10.2136/sssaj1980.03615995004400050002x.
- VanderKwaak, J. E. (1999), Numerical simulation of flow and chemical transport in integrated surface-subsurface hydrologic systems, Ph.D. dissertation, 217 pp., Univ. of Waterloo, Waterloo, Ont., Canada.
- VanderKwaak, J. E., and K. Loague (2001), Hydrologic-response simulations for the R-5 catchment with a comprehensive physics-based model, *Water Resour. Res.*, *37*, 999–1013, doi:10.1029/2000WR900272.
- Vereecken, H., R. Kasteel, J. Vanderborght, and T. Harter (2007), Upscaling hydraulic properties and soil water flow processes in heterogeneous soils: A review, *Vadose Zone J.*, *6*, 1–28, doi:10.2136/vzj2006.0055.
- Vivoni, E. R., V. Y. Ivanov, R. L. Bras, and D. Entekhabi (2005), On the effects of triangulated terrain resolution on distributed hydrologic model response, *Hydrol. Processes*, *19*, 2101–2122, doi:10.1002/hyp.5671.
- Vivoni, E. R., D. Entekhabi, R. L. Bras, and V. Y. Ivanov (2007), Controls on runoff generation and scale-dependence in a distributed hydrologic model, *Hydrol. Earth Syst. Sci.*, *11*(5), 1683–1701, doi:10.5194/hess-11-1683-2007.
- Wemple, B. C. (1998), Investigations of runoff production and sedimentation on forest roads, Ph.D. dissertation, 168 pp., Oreg. State Univ., Corvallis.
- Western, A. W., and R. B. Grayson (1998), The Tarrawarra data set: Soil moisture patterns, soil characteristics and hydrological flux measurements, *Water Resour. Res.*, *34*, 2765–2768, doi:10.1029/98WR01833.
- 
- B. A. Ebel, Water Resources Division, U.S. Geological Survey, 3215 Marine St., Ste. E-127, Boulder, CO 80303, USA.
- C. S. Heppner, Erler and Kalinowski, Inc., 1870 Ogden Dr., Burlingame, CA 94010, USA.
- K. Loague, Department of Geological and Environmental Sciences, Stanford University, Stanford, CA 94305-2115, USA.
- B. B. Mirus, U.S. Geological Survey, 345 Middlefield Rd., MS 420, Menlo Park, CA 94025, USA. (bbmirus@usgs.gov)